

Synthesis and electrochemical performance of 5V spinel $\text{LiNi}_{0.5}\text{Mn}_{1.5}\text{O}_4$ prepared by solid-state reaction

SUN Qiang(孙 强), LI Xin-hai(李新海), WANG Zhi-xing(王志兴), JI Yong(季 勇)

School of Metallurgical Science and Engineering, Central South University, Changsha 410083, China

Received 24 March 2008; accepted 3 June 2008

Abstract: Spinel compound $\text{LiNi}_{0.5}\text{Mn}_{1.5}\text{O}_4$ with high capacity and high rate capability was synthesized by solid-state reaction. At first, $\text{MnCl}_2 \cdot 4\text{H}_2\text{O}$ and $\text{NiCl}_2 \cdot 6\text{H}_2\text{O}$ were reacted with $(\text{NH}_4)_2\text{C}_2\text{O}_4 \cdot \text{H}_2\text{O}$ to produce a precursor via a low-temperature solid-state route, then the precursor was reacted with Li_2CO_3 to synthesize $\text{LiNi}_{0.5}\text{Mn}_{1.5}\text{O}_4$. The effects of calcination temperature and time on the physical properties and electrochemical performance of the products were investigated. Samples were characterized by thermal gravimetric analysis(TGA), scanning electron microscopy(SEM), X-ray diffractometry(XRD), charge-discharge tests and cyclic voltammetry measurements. Scanning electron microscopy(SEM) image shows that as calcination temperature and time increase, the crystallinity of the samples is improved, and their grain sizes are obviously increased. It is found that $\text{LiNi}_{0.5}\text{Mn}_{1.5}\text{O}_4$ calcined at $800\text{ }^\circ\text{C}$ for 6 h exhibits a typical cubic spinel structure with a space group of $Fd\bar{3}m$. Electrochemical tests demonstrate that the sample obtained possesses high capacity and excellent rate capability. When being discharged at a rate as high as $5C$ after 30 cycles, the as-prepared $\text{LiNi}_{0.5}\text{Mn}_{1.5}\text{O}_4$ powders can still deliver a capacity of $101\text{ mA}\cdot\text{h/g}$, which shows to be a potential cathode material for high power batteries.

Key words: lithium ion battery; $\text{LiNi}_{0.5}\text{Mn}_{1.5}\text{O}_4$; cathode; solid-state reaction

1 Introduction

High energy and high power rechargeable Li-ion cells are key components of the portable, entertainment, computing and hybrid electric vehicles[1–2]. One approach of increasing the power density of lithium ion batteries is to enhance its operation voltage by utilizing high-voltage cathodes. Transition metal-substituted spinel materials ($\text{LiM}_x\text{Mn}_{2-x}\text{O}_4$, $M=\text{Cr, Co, Fe, Ni, Cu}$) showed high voltage plateau at around 5V [3–7], and hence have been widely studied for advanced lithium ion batteries. The capacity and voltage plateau in $\text{Li}/\text{LiM}_x\text{Mn}_{2-x}\text{O}_4$ cells strongly depend on the kind of transition metals(M) and their contents. Among those materials, $\text{LiNi}_{0.5}\text{Mn}_{1.5}\text{O}_4$ received great attention for its dominant potential plateau at around 4.7 V . Moreover, $\text{LiNi}_{0.5}\text{Mn}_{1.5}\text{O}_4$ showed the highest discharge capacity ($146.7\text{ mA}\cdot\text{h/g}$) with stable cycleability at this high potential.

In recent years, many methods to synthesize $\text{LiNi}_{0.5}\text{Mn}_{1.5}\text{O}_4$ have been reported, including solid-state

method[8], sol-gel method[9], co-precipitation method [10], composite carbonate process[11], molten salt method[12], emulsion drying method[13], and ultrasonic spray pyrolysis method[14]. Different synthesizing methods can result in products with different properties[15]. In synthesized $\text{LiNi}_{0.5}\text{Mn}_{1.5}\text{O}_4$, secondary phases such as NiO and $\text{Li}_x\text{Ni}_{1-x}\text{O}$ usually exist in the products, which is due to the oxygen loss at high temperature and can deteriorate electrochemical behaviors[16]. Fortunately, the oxygen loss occurring at high temperatures can be mostly recovered by low rate cooling in low temperature annealing[17–18]. In this work, an improved preparation of $\text{LiNi}_{0.5}\text{Mn}_{1.5}\text{O}_4$ by solid reaction in air is described, and the electrochemical properties of resulting powders are studied.

2 Experimental

Appropriate amounts of chemicals, $\text{NiCl}_2 \cdot 6\text{H}_2\text{O}$ and $\text{MnCl}_2 \cdot 4\text{H}_2\text{O}$, were thoroughly mixed (cationic ratio of Ni to Mn of 1:3). Subsequently, 20% (mass fraction) excess of $(\text{NH}_4)_2\text{C}_2\text{O}_4 \cdot \text{H}_2\text{O}$ was added to the mixture, then the

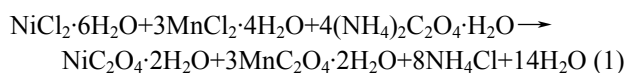
mixture was ground for about 0.5 h to ensure complete reaction. The obtained mixture was dried in air at 120 °C for 10 h and then was calcined at 400 °C for 3 h in air to form a precursor containing Ni and Mn (Ni-Mn for short). In order to investigate the effects of calcination temperature and calcination time on the physical properties and electrochemical performance of the products, the precursor was calcined at 750–900 °C for different time after being mixed with stoichiometric Li_2CO_3 , then kept at 600 °C for 24 h in air to obtain products.

Thermogravimetric(TG) analysis was performed on a thermogravimetric analyzer (Universal V4.0C TA Instruments: SDT Q600 V8.0 Build 95) at a heating rate of 10 °C/min in a constant flow of extra dry air at 100 mL/min. The powder X-ray diffraction (XRD, Rint-2000, Rigaku) measurement using Cu K_α radiation was employed to identify the crystalline phase of the synthesized materials. The particle size and morphology of $\text{LiNi}_{0.5}\text{Mn}_{1.5}\text{O}_4$ powders were observed by scanning electron microscope (SEM, JEOL, JSM-5600LV) with an accelerating voltage of 20 kV.

The electrochemical properties of the products were tested in cells with metallic lithium as anode electrode. For cathode fabrication, the prepared powders were mixed with 10% acetylene black and 10% polyvinylidene fluoride in *N*-methyl pyrrolidinone(NMP) until a slurry was obtained. And then, the blended slurries were pasted onto an aluminum current collector, and the electrode was dried at 120 °C for 10 h in vacuum. The test cell consisted of the cathode and lithium foil anode separated by a porous polypropylene film, and the electrolyte solution was 1 mol/L LiPF_6 in a mixture of ethylene carbonate(EC), ethyl methyl carbonate(EMC) and dimethyl carbonate(DMC) in a volume ratio of 1:1:1. The assembly of the cells was carried out in a dry Ar-filled glove box. The cells were charged and discharged over a voltage range of 3.5–4.9 V versus Li/Li^+ electrode at room temperature. Cyclic voltammogram was measured at a sweep rate of 0.1 mV/s between 3.5 and 5.2 V.

3 Results and discussion

In the preparation of Ni-Mn precursor via a low-temperature solid-state route, the following reaction could take place[19]:



Since the reaction was performed at room temperature, the mixture obtained may contain plenty of nanosized oxalate compounds. It is well known that oxalate compounds often have low decomposition

temperature, thus it is highly possible to synthesize $\text{LiNi}_{0.5}\text{Mn}_{1.5}\text{O}_4$ by simply calcining the precursor at low temperatures.

Thermogravimetry(TG) analysis tests for oxalate compound of Ni-Mn and the mixture of Ni-Mn precursor and Li_2CO_3 were carried out, respectively. The TG curve for oxalate compound is shown in Fig.1(a). The mass loss terminates at about 400 °C, and two discrete mass losses are observed due to removal of water at 25–280 °C and the decomposition of oxalate compound of Ni-Mn at 280–400 °C. When the temperature goes up beyond 400 °C, just small mass losses are observed, which indicates that a properly stable Ni-Mn oxide is obtained. In order to save energy, based on the TG data, a calcining temperature of 400 °C is used to prepare the Ni-Mn precursor. After being mixed with stoichiometric Li_2CO_3 , the Ni-Mn precursor shows three mass losses, as indicated in Fig.1(b). Mass losses below 600 °C are associated with the water release and pyrolysis of the Li_2CO_3 , while no mass loss is observed between 600 °C and 780 °C, which indicates that the water and CO_2 have been released completely below 600 °C. However, when the temperature increases to 780 °C, a third mass loss occurs, which is likely caused by oxygen loss. The oxygen content in the ambient atmosphere is expected to play an important role in the stability of the cubic spinel.

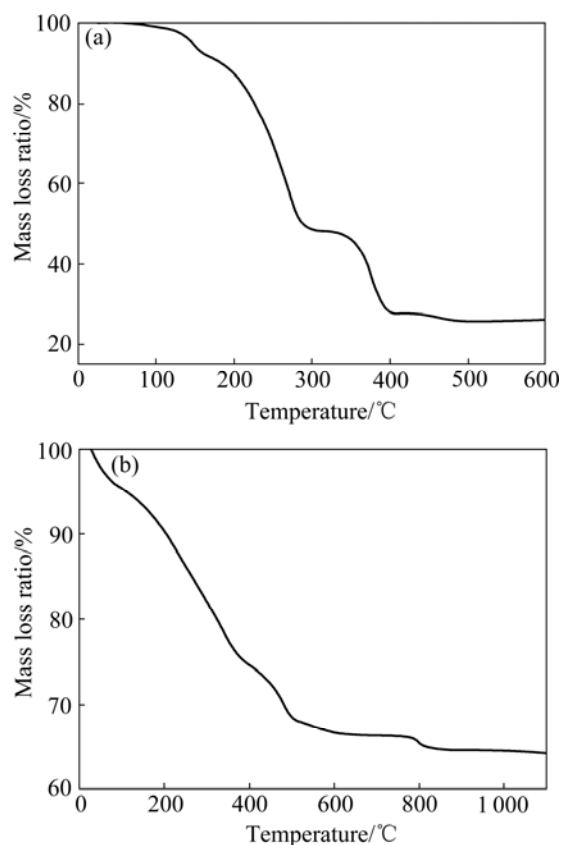


Fig.1 TG curves for oxalate compound of Ni-Mn (a) and Ni-Mn precursor mixed with Li_2CO_3 (b)

It is proved that the strategy of slow cooling or annealing treatment at low temperature is very necessary to optimize the oxygen content of $\text{LiNi}_{0.5}\text{Mn}_{1.5}\text{O}_4$ because the oxygen loss of $\text{LiNi}_{0.5}\text{Mn}_{1.5}\text{O}_4$ occurs at high temperature[17]. Therefore, annealing at 600 °C for 20 h is introduced in order to compensate for oxygen loss.

Fig.2 shows the XRD patterns of $\text{LiNi}_{0.5}\text{Mn}_{1.5}\text{O}_4$ powders obtained after calcining at different temperatures for 6 h. All samples are confirmed as a typical cubic spinel structure with a space group of $Fd\bar{3}m$. As the calcination temperature increases from 750 to 900

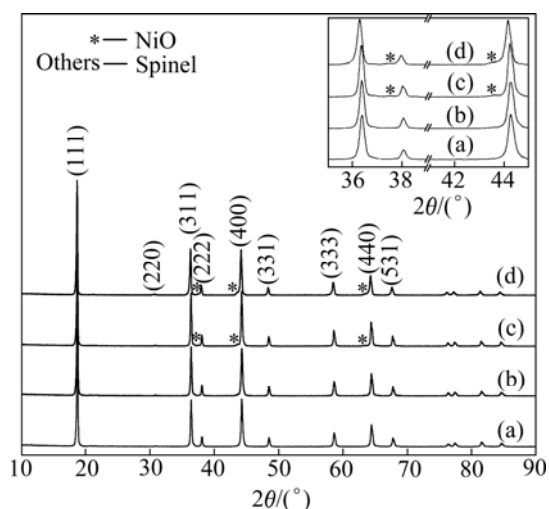


Fig.2 XRD patterns of $\text{LiNi}_{0.5}\text{Mn}_{1.5}\text{O}_4$ powders calcined at different temperatures for 6 h: (a) 750 °C; (b) 800 °C; (c) 850 °C; (d) 900 °C

°C, the diffraction peaks become sharper and stronger, indicating that the crystallinity is improved. It is noted that as the calcination temperature increases to 850 °C, the slight peaks representing NiO impurities appear on the left of the (222), (400) and (440) peaks in the XRD pattern, as shown in Fig.2.

The morphologies of $\text{LiNi}_{0.5}\text{Mn}_{1.5}\text{O}_4$ powders obtained at various temperatures were observed using a SEM, and the results are shown in Fig.3. It can be seen that 750 °C-calcined sample displays undeveloped crystallization and a little agglomeration. As calcination temperature increases, the grain size grows obviously, and 900 °C-calcined sample has the maximum particle size (approximate 2.5 μm). This implies a sharp decline in the specific surface area of the samples as calcination temperature is elevated. It is also found that the samples calcined at the temperatures higher than 800 °C represent clear polyhedral shape, indicating well-developed crystallinity. These are in the agreement with the results from XRD.

The charge and discharge curves of $\text{LiNi}_{0.5}\text{Mn}_{1.5}\text{O}_4$ powders prepared at different temperatures are shown in Fig.4, which are carried out at current density of 0.2C (C represents 1 Li^+ ion exchanged in 1 h equivalent to 148 mA/g). It can be seen that its discharge capacity increases with the calcination temperature increasing under 800 °C. This may originate from relatively higher crystallinity of 800 °C-calcined sample and less electrolyte decomposition products formed on the sur-

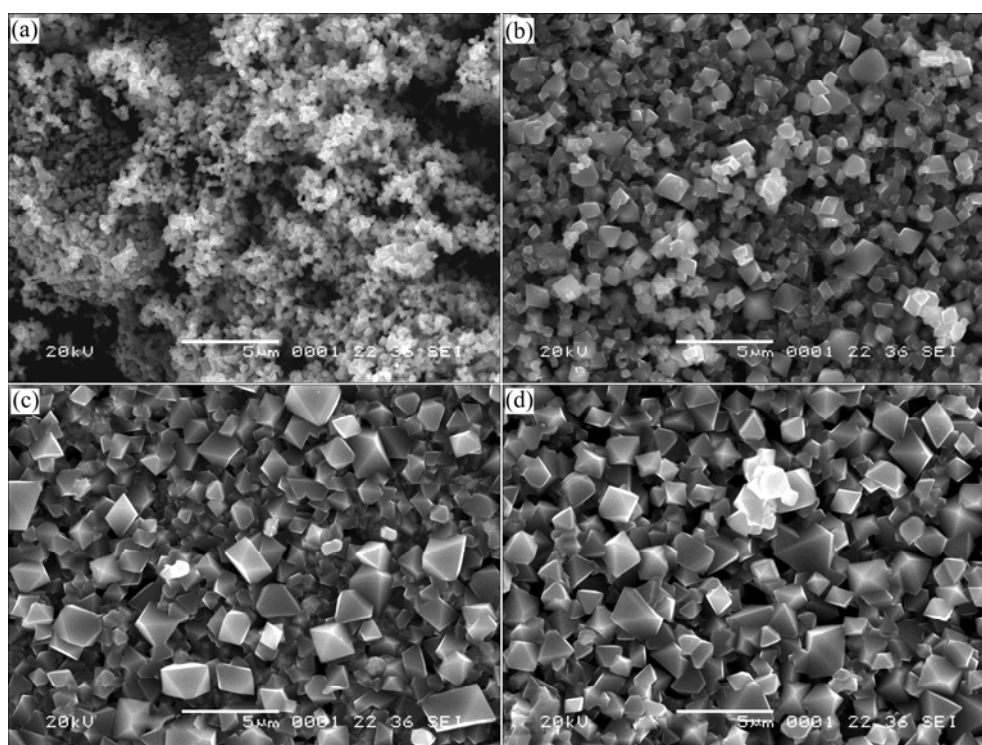


Fig.3 SEM images of $\text{LiNi}_{0.5}\text{Mn}_{1.5}\text{O}_4$ products obtained by calcining at different temperatures for 6 h: (a) 750 °C; (b) 800 °C; (c) 850 °C; (d) 900 °C

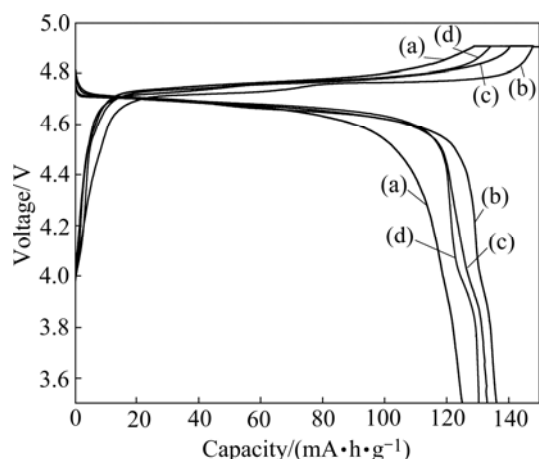


Fig.4 Charge and discharge curves of $\text{LiNi}_{0.5}\text{Mn}_{1.5}\text{O}_4$ prepared by calcining at different temperatures for 6 h: (a) 750 °C; (b) 800 °C; (c) 850 °C; (d) 900 °C

faces of this sample. When the temperature increases beyond 850 °C, the discharge capacity shows a little decline. This is closely related to the high calcination temperature employed (>800 °C) which may result in the presence of undesired impurities such as NiO or $\text{Li}_x\text{Ni}_{1-x}\text{O}$ in the final product, and these impurities may, to a great extent, deteriorate the electrochemical performance of $\text{LiNi}_{0.5}\text{Mn}_{1.5}\text{O}_4$. It is noted that the discharge curves of 850 °C- and 900 °C-calcined samples still present shorter plateaus in the potential region from 3.9C to 4.2C besides the higher plateaus of around 4.7 V, which results from the transfer reaction between Mn^{3+} and Mn^{4+} . It can also be seen from Fig.4 that the samples calcined at relatively higher temperatures (800–900 °C) have much larger initial discharge capacities (>130 mA·h/g) than those calcined at lower temperatures (750 °C, 125 mA·h/g), although the lower discharge plateaus occur due to the existence of Mn^{3+} ions.

The XRD patterns of $\text{LiNi}_{0.5}\text{Mn}_{1.5}\text{O}_4$ powders calcined at 800 °C for different time are shown in Fig.5. It is seen that all diffraction peaks of three samples are ascribed to a cubic spinel structure with a space group of $Fd\bar{3}m$. As the calcination time increases, the diffraction peaks become sharper and stronger. When products are calcined for 12 h, some diffraction peaks of impurities are observed, which indicates that there are some impurities, such as NiO or $\text{Li}_x\text{Ni}_{1-x}\text{O}$. Fig.6 shows the SEM images of as-prepared samples. It can be seen that the particles grow up from 0.5, 1 to 2.5 μm with increasing the calcination time from 1, 6 to 12 h. When samples are calcined for more time, such as 6 h and 12 h, the clearer octahedral shape characteristic of cubic spinel is observed, indicating the well-developed crystallinity.

The charge-discharge curves of as-prepared $\text{LiNi}_{0.5}\text{Mn}_{1.5}\text{O}_4$ cycled between 3.5 V and 4.9 V at the rate of 0.2C are shown in Fig.7. It is seen that the calcina-

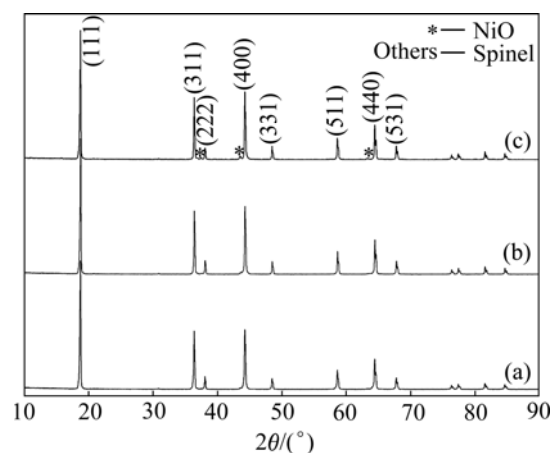


Fig.5 XRD patterns of $\text{LiNi}_{0.5}\text{Mn}_{1.5}\text{O}_4$ powders obtained by calcining at 800 °C for different time: (a) 1 h; (b) 6 h; (c) 12 h

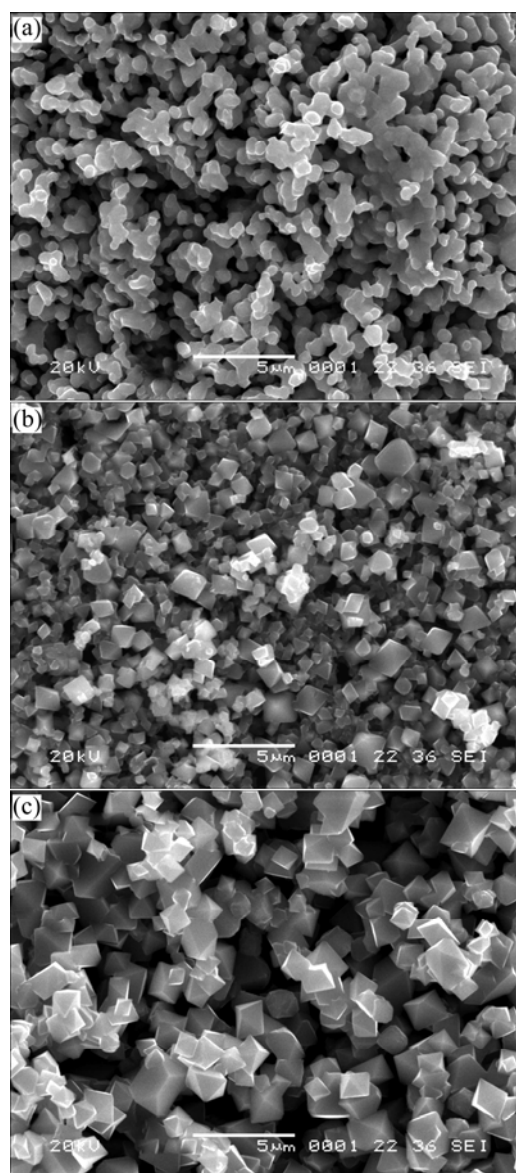


Fig.6 SEM images of $\text{LiNi}_{0.5}\text{Mn}_{1.5}\text{O}_4$ powders obtained by calcining at 800 °C for different time: (a) 1 h; (b) 6 h; (c) 12 h

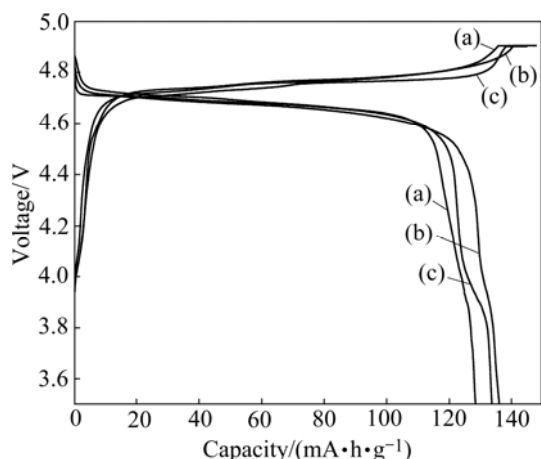


Fig.7 Charge and discharge curves of $\text{LiNi}_{0.5}\text{Mn}_{1.5}\text{O}_4$ powders calcined at $800\text{ }^\circ\text{C}$ for different time: (a) 1 h; (b) 6 h; (c) 12 h

tion time has a significant effect on the charge-discharge profiles of $\text{LiNi}_{0.5}\text{Mn}_{1.5}\text{O}_4$. When being calcined at $800\text{ }^\circ\text{C}$ for 1 h, $\text{LiNi}_{0.5}\text{Mn}_{1.5}\text{O}_4$ shows only one plateau at around 4.7 V, which demonstrates that most of lost oxygen is already recovered by annealing process. When the calcination time is more than 6 h, $\text{LiNi}_{0.5}\text{Mn}_{1.5}\text{O}_4$ materials exhibit two plateaus at around 4.7 V and 4 V, which are attributed to the $\text{Ni}^{2+}/\text{Ni}^{4+}$ and $\text{Mn}^{3+}/\text{Mn}^{4+}$ redox couples, respectively. Moreover, as the calcination time reaches 12 h, there is a clearer discharging plateau at around 4 V than that of 6 h. This indicates that even though annealing process is employed for 12 h, the products could not compensate for the oxygen loss. In addition, the discharge capacity increases from 128 to 136 $\text{mA}\cdot\text{h}/\text{g}$ with increasing the calcination time from 1 to 6 h. This observation can be understood in terms of the optimized crystallinity in the final product after calcining for a relative long time. 6 h- and 12 h-calcined $\text{LiNi}_{0.5}\text{Mn}_{1.5}\text{O}_4$ samples show almost equal capacity when being discharged at the rate of 0.2C, but the capacity of 12 h-calcined $\text{LiNi}_{0.5}\text{Mn}_{1.5}\text{O}_4$ (133 $\text{mA}\cdot\text{h}/\text{g}$) is slightly smaller than that of 6 h-calcined sample. This behavior is most likely associated with the increased amount of Mn^{3+} and NiO impurities which caused by oxygen deficiency after long calcination treatment.

In Fig.8 the cyclic voltammetry(CV) curves of $\text{LiNi}_{0.5}\text{Mn}_{1.5}\text{O}_4$ samples prepared under optimization conditions (calcining at $800\text{ }^\circ\text{C}$ for 6 h) are plotted in the potential range from 3.5 V to 5.2 V at a scanning rate of 0.1 mV/s. The major doublet redox peaks at around 4.5–5 V originate from the $\text{Ni}^{2+}/\text{Ni}^{4+}$ redox couple and the ordering of lithium on 8a sites at 50% filling[16]. Whereas the small doublet redox peaks in the potential region from 3.9 to 4.2 V are ascribed to the $\text{Mn}^{3+}/\text{Mn}^{4+}$ redox, which results from the existence of small amount of NiO or $\text{Li}_x\text{Ni}_{1-x}\text{O}$ impurities in the sample. With the increase of the charge-discharge cycles, the major

doublet redox peaks at around 4.5–5V of the sample gradually overlap, and become a little broad peak after 30 cycles. At the same time, the potential difference between the oxidation and reduction peaks gets smaller, and the reduction-peak currents slightly increase. This indicates that the electrochemical reversibility and activity of the product increase with the increase of charge-discharge cycle, and the corresponding electrode polarization decreases. The results of CV experiments are in good agreement with those of the preceding charge-discharge experiments.

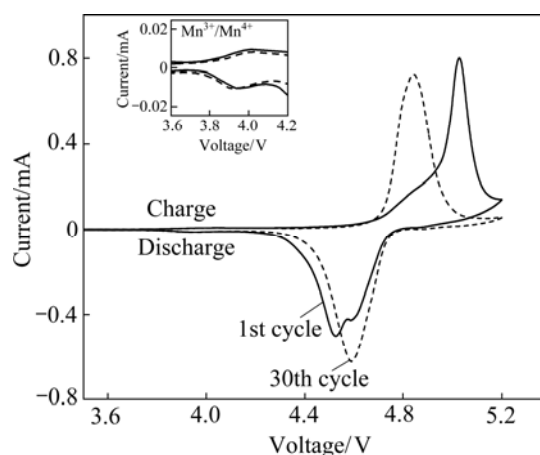


Fig.8 Cyclic voltammetry curves of $\text{LiNi}_{0.5}\text{Mn}_{1.5}\text{O}_4$ sample obtained by calcining at $800\text{ }^\circ\text{C}$ for 6 h (Scanning rate 0.1 mV/s, potential 3.5–5.2 V)

It is well-known that rate capability plays an important role in lithium ion batteries. Here, high-rate electrochemical performance of $\text{LiNi}_{0.5}\text{Mn}_{1.5}\text{O}_4$ prepared under optimization conditions (calcining at $800\text{ }^\circ\text{C}$ for 6 h) was evaluated. Fig.9 shows cycling performance of $\text{LiNi}_{0.5}\text{Mn}_{1.5}\text{O}_4$ cycled between 3.5 and 4.9 V, charged at the rate of 0.1C and discharged at the 0.2C, 1C and 5C

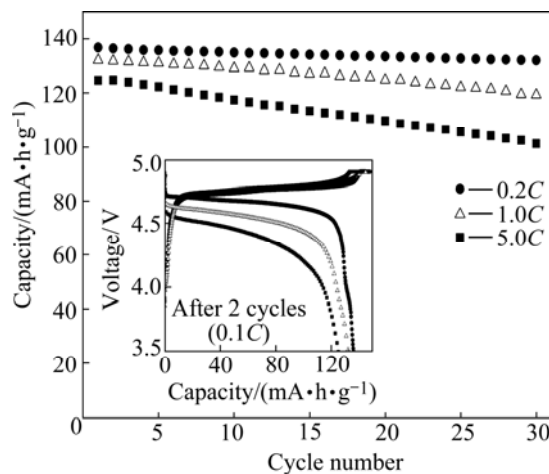


Fig.9 Cycle performances of $\text{LiNi}_{0.5}\text{Mn}_{1.5}\text{O}_4$ powders calcined at $800\text{ }^\circ\text{C}$ for 6 h

for 30 times, respectively. Before comparison of high-rate test, the cell was charge-discharged at a rate of 0.1C in a voltage range of 3.5–4.9 V for two times. It can be seen that both the plateau voltage and the discharge capacity decrease with the current density increasing. The product shows a considerable stable cycling behavior and the cycling retention rate after 30 cycles is over 96% at low current density of 0.2C. When the current density increases to 1C and 5C, although the samples exhibit an inferior cycling behavior, the cycling retention rates of products after 30 cycles can still reach 90% and 81%, respectively. Therefore, it can be concluded that as-prepared products possess excellent electrochemical performance even at high rate.

4 Conclusions

1) $\text{LiNi}_{0.5}\text{Mn}_{1.5}\text{O}_4$ products can be classified as the typical cubic spinel $Fd\bar{3}m$ structure with simple phase. Sample characterizations indicate that the crystallinity and morphology of the products can be improved by increasing the calcination temperature and time.

2) The electrochemical performance measurements demonstrate that $\text{LiNi}_{0.5}\text{Mn}_{1.5}\text{O}_4$ products calcined at 800 °C for 6 h have much improved capacity and excellent rate capability. The discharge capacity reaches up to 136 mA·h/g at a current density of 0.2C, while it retains as high as 101 mA·h/g even at a high current density of 5C after 30 cycles.

References

- [1] YOSHIO N. Lithium ion secondary batteries: Past 10 years and the future [J]. *Journal of Power Sources*, 2001, 100: 101–106.
- [2] LIU Li-ying, TIAN Yan-wen, ZHAI Yu-chun, XU Cha-qing. Influence of Y^{3+} doping on structure and electrochemical performance of layered $\text{Li}_{1.05}\text{V}_3\text{O}_8$ [J]. *Trans Nonferrous Met Soc China*, 2007, 17(1): 110–115.
- [3] MOLEND A J, MARZEC J, SWIERCZEK K, OJCZUK W, ZIEMNICKI M, MOLEND A M, DROZDEK M, DZIEMBAU R. The effect of 3d substitutions in the manganese sublattice on the charge transport mechanism and electrochemical properties of manganese spinel [J]. *Solid State Ionics*, 2004, 171: 215–227.
- [4] OHZUKU T, TAKEDA S, IWANAGA M. Solid-state redox potentials for $\text{Li}[\text{Me}_{1/2}\text{Mn}_{3/2}]\text{O}_4$ (Me: 3d-transition metal) having spinel-framework structures: A series of 5 volt materials for advanced lithium-ion batteries [J]. *Journal of Power Sources*, 1999, 81/82: 90–94.
- [5] OHZUKU T, ARIYOSHI K, TAKEDA S, SAKAI Y. Synthesis and characterization of 5V insertion material of $\text{Li}[\text{Fe}_x\text{Mn}_{2-x}]\text{O}_4$ for lithium-ion batteries [J]. *Electrochimica Acta*, 2001, 46: 2327–2336.
- [6] BONINO F, PANERO S, SATOLLI D, SCROSATI B. Synthesis and characterization of $\text{Li}_2\text{M}_x\text{Mn}_{4-x}\text{O}_8$ (M=Co, Fe) as positive active materials for lithium-ion cells [J]. *Journal of Power Sources*, 2001, 97/98: 389–392.
- [7] TERADA Y, YASAKA K, NISHIKAWA F, KONISHI T, YOSHIO M, NAKAI I. In situ XAFS analysis of $\text{Li}(\text{Mn}, \text{M})_2\text{O}_4$ (M=Cr, Co, Ni) 5V cathode materials for lithium-ion secondary batteries [J]. *Journal of Solid State Chemistry*, 2001, 156: 286–291.
- [8] FANG Hai-sheng, WANG Zhi-xing, LI Xin-hai, GUO Hua-jun, PENG Wen-jie. Exploration of high capacity $\text{LiNi}_{0.5}\text{Mn}_{1.5}\text{O}_4$ synthesized by solid-state reaction [J]. *Journal of Power Sources*, 2006, 153: 174–176.
- [9] ANDOUNI N, ZAGHIB K, GENDRON F, MAUGER A, JULIEN C M. Magnetic properties of $\text{LiNi}_{0.5}\text{Mn}_{1.5}\text{O}_4$ spinels prepared by wet chemical methods [J]. *Journal of Magnetism and Magnetic Materials*, 2007, 309: 100–105.
- [10] FAN Yu-kai, WANG Jian-ming, YE Xue-bo, ZHANG Jian-qing. Physical properties and electrochemical performance of $\text{LiNi}_{0.5}\text{Mn}_{1.5}\text{O}_4$ cathode material prepared by a coprecipitation method [J]. *Materials Chemistry and Physics*, 2007, 103: 19–23.
- [11] LIU G Q, WANG Y J, QI L, LI W, CHEN H. Synthesis and electrochemical performance of $\text{LiNi}_{0.5}\text{Mn}_{1.5}\text{O}_4$ spinel compound [J]. *Electrochimica Acta*, 2005, 50: 1965–1968.
- [12] KIM J H, MYUNG S T, SUN Y K. Molten salt synthesis of $\text{LiNi}_{0.5}\text{Mn}_{1.5}\text{O}_4$ spinel for 5V class cathode material of Li-ion secondary battery [J]. *Electrochimica Acta*, 2004, 49: 219–227.
- [13] MYUNG S T, KOMABA S, KUMAGAI N, YASHIRO H, CHUNG H T, CHO T H. Nano-crystalline $\text{LiNi}_{0.5}\text{Mn}_{1.5}\text{O}_4$ synthesized by emulsion drying method [J]. *Electrochimica Acta*, 2002, 47: 2543–2549.
- [14] PARK S H, SUN Y K. Synthesis and electrochemical properties of 5V spinel $\text{LiNi}_{0.5}\text{Mn}_{1.5}\text{O}_4$ cathode materials prepared by ultrasonic spray pyrolysis method [J]. *Electrochimica Acta*, 2004, 50: 431–434.
- [15] ARREBOLA J C, CABALLERO A, CRUZ M. Crystallinity control of a nanostructured $\text{LiNi}_{0.5}\text{Mn}_{1.5}\text{O}_4$ spinel via polymer-assisted synthesis: A method for improving its rate capability and performance in 5V lithium batteries [J]. *Adv Funct Mater*, 2006, 16: 1904–1912.
- [16] ALCANTARA R, JARABA M, LAVELA P, TIRADA J L. Optimizing preparation conditions for 5V electrode performance, and structural changes in $\text{Li}_{1-x}\text{Ni}_{0.5}\text{Mn}_{1.5}\text{O}_4$ spinel [J]. *Electrochimica Acta*, 2002, 47: 1829–1835.
- [17] ZHANG Bao, WANG Zhi-xing, GUO Hua-jun. Effect of annealing treatment on electrochemical property of $\text{LiNi}_{0.5}\text{Mn}_{1.5}\text{O}_4$ spinel [J]. *Trans Nonferrous Met Soc China*, 2007, 17(2): 287–290.
- [18] FANG Hai-sheng, WANG Zhi-xing, ZHANG Bao, LI Xin-hai, LI Guang-she. High performance $\text{LiNi}_{0.5}\text{Mn}_{1.5}\text{O}_4$ cathode materials synthesized by a combinational annealing method [J]. *Electrochemistry Communications*, 2007, 9: 1077–1082.
- [19] FANG Hai-sheng, LI Li-ping, LI Guang-she. A low-temperature reaction route to high rate and high capacity $\text{LiNi}_{0.5}\text{Mn}_{1.5}\text{O}_4$ [J]. *Journal of Power Sources*, 2007, 167: 223–227.

(Edited by YANG Bing)